Eur Radiol (2011) 21:1233–1242
DOI 10.1007/s00330-010-2030-1

MAGNETIC RESONANCE

Contribution of the hepatobiliary phase of Gd-EOB-DTPA-enhanced MRI to Dynamic MRI in the detection of hypovascular small (≤2 cm) HCC in cirrhosis

Rita Golfieri · Matteo Renzulli · Vincenzo Lucidi · Beniamino Corcioni · Franco Trevisani · Luigi Bolondi

Received: 23 June 2010 / Revised: 15 September 2010 / Accepted: 20 October 2010 / Published online: 5 February 2011

Abstract
Objective To prospectively assess the additional value of the hepatobiliary (HB) phase of Gd-EOB-DTPA-MRI in identifying and characterising small (≤2 cm) hepatocellular carcinomas (HCCs) undetermined in dynamic phases alone because of their atypical features, according to the AASLD criteria.
Methods 127 cirrhotic patients were evaluated with Gd-EOB-DTPA-MRI in two sets: unenhanced and dynamic phases; unenhanced, dynamic and HB phases. Sixty-two out of 215 nodules (29%) were atypical in 42 patients (33%).
Results 62 atypical nodules were reported at histology: high-grade dysplastic nodules (HGDN)/early HCC (n=20), low-grade DN (LGDN) (n=21), regenerative nodules (n=17) and nodular regenerative hyperplasia (n=4). The sensitivity, specificity, accuracy, positive and negative predictive value (PPV, NPV) were increased by the addition of the HB phase: 88.4–99.4%, 88–95%, 88–98.5%, 97–99%, and 65–97.5%, respectively. Twenty atypical nodules were malignant (32%), 19 of which were characterised only during the HB phase.
Conclusions The HB phase is 11% more sensitive in the classification of HGDN/early HCC than dynamic MRI, with an added value of 32.5% in the NPV. The high incidence (33%) of atypical nodules and their frequent malignancy (32%) suggest the widespread employment of Gd-EOB-DTPA-MRI in the follow-up of small nodules (≤2 cm) in cirrhosis.

Keywords Hypovascular HCC · Atypical small liver nodules · Cirrhosis · Gd-EOB-DTPA-enhanced MR imaging · Magnetic resonance imaging

R. Golfieri (✉) · M. Renzulli · V. Lucidi · B. Corcioni
Radiology Unit, Department of Digestive Diseases and Internal Medicine, Sant'Orsola-Malpighi Hospital, University of Bologna, Bologna, Italy
e-mail: rita.golfieri@aosp.bo.it

F. Trevisani
Unit of Semeiotica, Department of Digestive Diseases and Internal Medicine, Sant'Orsola-Malpighi Hospital, University of Bologna, Bologna, Italy

L. Bolondi
Unit of Internal Medicine, Department of Digestive Diseases and Internal Medicine, Sant'Orsola-Malpighi Hospital, University of Bologna, Bologna, Italy

Introduction

Hepatocellular carcinoma (HCC) is the most frequent primary hepatic malignancy and the major cause of death in cirrhotic patients [1, 2]. Its incidence is increasing in most countries, and it represents a worldwide health problem [3–5].

Multi Detector-row CT (MDCT) is the most widely used imaging technique for HCC detection and staging. However, state-of-the-art 3D Gadolinium-enhanced dynamic MRI is considered more sensitive than MDCT and is increasingly used for the detection and characterisation of small hepatic nodules [6–8]. Both techniques reveal HCCs based on their altered arterial vascularity due to the development of unpaired arteries and sinusoidal capillarisation [9–12]. Enhancement in the arterial phase and washout in the portal venous and delayed phases are now regarded as distinctive features of HCC in liver cirrhosis. According to the recently revised American Association for the Study of Liver

Diseases (AASLD) criteria, for lesions >1 cm a single dynamic imaging study (4-phase MDCT scan or dynamic MRI) showing this typical vascular pattern is enough to confirm the diagnosis of HCC, whereas for <1 cm nodules an ultrasound (US) follow-up at 3-month intervals is recommended, to detect their increase in size or a change in vascular pattern [13–15].

However, in small (≤2 cm) nodules an atypical vascular profile is not uncommon, challenging the definitive radiological diagnosis: these lesions may, in fact, be either early HCCs or preneoplastic lesions, such as high-grade dysplastic nodules (HGDN) [16–18].

After Gadobenate dimeglumine (Gd-BOPTA), gadoxetic-acid-disodium (Gd-EOB-DTPA) is the second generation hepatocytes-directed gadolinium-based paramagnetic contrast agent, which has been available in Europe since 2004. These contrast media are named "dual agents" as they combine the properties of a conventional extracellular contrast agent with those of a liver-specific contrast agent [19–24]. After a dynamic phase, Gd-EOB-DTPA accumulates in functioning hepatocytes in the delayed phase which begins earlier than with Gd-BOPTA (10 mins after injection) and undergoes hepatobiliary excretion at a high rate (50%) with potentially stronger liver enhancement and more pronounced hypointensity of malignancies.

However, only a few studies have been conducted using hepatobiliary MRI contrast agents to determine the enhancement pattern of small atypical lesions occurring in cirrhotic livers, in order to define their nature [24–27].

The purpose of this prospective study was to assess the additional value of the hepatobiliary (HB) phase of Gd-EOB-DTPA-enhanced MRI in identifying and characterising small (≤2 cm) histologically confirmed HCCs occurring in cirrhosis and unclassified at dynamic phases because of their atypical features.

Materials and methods

Patients

This prospective study, compliant with the Declaration of Helsinki principles [28], was performed at a "tertiary liver care" centre. The study protocol was approved by the Ethics committee of our institute. All patients gave their written informed consent. Between May 2008 and October 2009, 127 male patients (91 [71.5%], mean age 54 years [range 31–77] with alcoholic [n=18] or HBV/HCV-related cirrhosis [n=44/65]), underwent Gd-EOB-DTPA-enhanced MRI to characterize small (≤2 cm) HCC nodules detected as suspicious during a US-surveillance program. All nodules showing an increase in size and the newly appeared lesions were evaluated with CEUS—performed in the same US session—and subsequently with MDCT. All uncertain and/or discrepant findings in >1 cm nodules at CEUS and MDCT were recruited for Gd-EOB-DTPA-enhanced MRI.

All patients bore at least 1 nodule measuring 1–2 cm and one or more incidental or satellite <1 cm nodules: 12 patients had solitary lesions, 5 two lesions, 2 three lesions, 4 five lesions, 2 six lesions, and the remaining patients had eight lesions.

Two hundred-fifteen nodules were identified at MRI (mean diameter 16 mm; range 4–20). Of them, 149 (69.3%) demonstrated a typical vascular pattern of HCC in 81 patients (38%) whereas 4 (2%) showed a "mosaic" HCC pattern in four patients (2%). Furthermore, 62 nodules (29%), with a mean diameter of 1.4 cm (range 8–19 mm) showing an *atypical vascular pattern* for HCC at dynamic MRI study were identified in 42 patients (33%) (Table 1).

All the 153 typical nodules had a histological confirmation after liver resection, transplantation or percutaneous biopsy preliminary to radio frequency (RF) ablation or were confirmed as an intense Lipodol uptake after transarterial chemoembolization (TACE). All 62 atypical nodules had histological confirmation on the surgical specimen after resection (n=32), transplantation (n=11) or whereby a US/CT-guided biopsy (n=19).

Histological diagnosis was performed by two expert pathologists in consensus reading as per the criteria outlined by the International Working Party [18, 29].

MR imaging

MR imaging was performed with a 1.5T superconducting system (Signa, GE Medical Systems, Milwaukee, WI, USA), using a body phased array multicoil for signal detection. Images were acquired in the axial plane, with a section thickness of 4 mm, an intersection gap of 0 mm, and a 28–35 cm field of view, with the exception of a three-dimensional breath-hold fast spoiled gradient-echo (GRE) sequence obtained after gadolinium-EOB-DTPA injection, acquired with a slice thickness of 4–5 mm, with an effective section thickness of 2–2.5 mm.

Unenhanced sequences were as follows:

- respiratory-triggered fat-suppressed fast recovery T2-weighted fast spin-echo (FR-FSE) (TR/TE 1500 to 1760/100, 256×190 matrix, 41.67 KHz per pixel bandwidth, 20–25 s acquisition time) or breath-hold T2-weighted single-shot FSE sequences (2.000/80 TR/TE, matrix 256/190), with and without fat saturation.
- breath-hold T1-weighted GRE dual-echo "in and out of phase" [TR/TE 150/4.6 and 150/2.1, respectively, 80° flip angle, a 256×160 matrix and 62.50 Hz per pixel bandwidth, 1 signal acquired, 20–25 s acquisition time].

Table 1 Nodules MR appearance according to the histological classes and the three-point classification scale (* - hypointensity; = isointensity; + hyperintensity)

Histology	Number	Range (mm)	HB phase appearance*	T2w	Typical dynamic and HB pattern	Atypical pattern Score 1	Atypical pattern Score 2	Atypical pattern Score 3
Overt HCC	153	7-20						
<1 cm	31	7–9	- n 31	+ n 14 =/- n 17	31			
1-2 cm	122	10–20	- n 122	+ n 93 =/- n 29	122			
HGDN-Early HCC	20							
<1 cm	2	8	- n 2	= n 2	–	2		
1–2 cm	18	10–20	- n 17 = n 1	+ n 1 =/- n 17		17	1	
RN-LGDN	38				–			
<1 cm	5	4–9	= n 5	=/- n 5			5	
1–2 cm	33	10–20	- n 2 = n 31	=/- n 33		2	31	
NRH	4	9–18			–			
<1 cm	1	9	+ n 1	=/- n 1				1
1–2 cm	3	12–18	+ n 3	+ n 2 =/- n 1				3
Total N. 215	Total N. 215				Total N. 153	Total N. 21	Total N. 37	Total N. 4

Contrast-enhanced sequences were acquired after intravenous (IV) injection of Gd-EOB-DTPA (Primovist, Bayer Schering Pharma AG, Berlin, Germany) at a dose of 0.1 ml/kg body weight (injection volume of 9–14 ml according to body weight) at a speed of 2 ml/sec immediately followed by a 20-mL saline flush through an antecubital venous catheter, using a dual power injector.

Both dynamic and HB-phase images were obtained using a fat-suppressed, 3D GRE sequence (Liver Acquisition with Volume Acceleration: LAVA, GE Medical Systems) before and after IV bolus administration of Gd-EOB-DTPA. Imaging delay times were determined with real-time MRI fluoroscopic monitoring after contrast agent administration. Hepatic arterial phase images were obtained 7 s after the arrival of contrast medium in the distal thoracic aorta, and portal venous and equilibrium phase images were obtained, respectively, 60 and 180 s after the beginning of the injection. Finally, HB-phase imaging was obtained 10 and 20 min after the beginning of contrast-medium injection.

Imaging analysis

Magnetic resonance images were divided in two datasets. Set 1 included the combined reading of unenhanced (basal T1-and T2-weighted) and Dynamic phase images (arterial-, portal venous- and equilibrium-phases); set 2 considered the unenhanced, Dynamic phases and HB-phases (10- and 20-min delayed images).

These two sets of MR images were evaluated by two radiologists (MR and VL), with more than 6 years' experience in liver MR imaging by a sequential reading (both radiologists read both sets within 15 days, to minimize reading bias). Any interpretation discrepancies were resolved by consensus with the participation of a third radiologist (RG).

The diagnosis of HCC was made according to the AASLD criteria for 1–2 cm nodules (hypervascularity in the arterial phase and washout in the portal venous/delayed phases) [13, 15], arbitrarily extending the same criterion also to the size range of <1 cm nodules. The nodules showing a "mosaic pattern" were also considered to be HCCs [30]. All nodules that did not fulfil these standards of reference were defined as *atypical nodules* and were classified according to the following criteria:

- HGDN/early HCC [31–33]: (a) nodule with arterial enhancement and hyperintensity on T2-weighted images and no uptake of contrast agent on HB images; (b) nodule with isointensity at Dynamic study, hyperintensity on T2-weighted images, and no uptake of contrast agent on HB images, or (c) nodule larger than 1.5 cm with absent uptake of contrast agent on HB-phase images.
- nodular regenerative hyperplasia (NRH)[34, 35]: (a) nodule with arterial enhancement and absent washout and (b) hyperintensity on HB-phases.
- regenerative nodules (RN) or low grade dysplastic nodules (LGDN): nodules that did not accomplish one of the previous criteria.

According to these criteria, the observers recorded the probable diagnosis for each atypical nodule by using the following *three-point classification scale*: score 1, probably HGDN/early HCC; score 2, probably RN/LGDN and score 3, probably NRH.

By comparing the scoring results with the standard of reference, we calculated the number of true-positive, true-negative, false-positive, and false-negative lesions for each observer. Benign lesions determined by the standard of reference constituted true-negative lesions.

Statistical analysis

Sensitivity, specificity, diagnostic accuracy, Positive and Negative Predictive Values (PPV/NPV) were calculated for the two sets of MR images for each observer.

The Chi-squared test was used to compare the sensitivities, specificities, diagnostic accuracies, PPV and NPV between the two sets of MR images, according to different nodule size ranges, and between the two observers. A two-tailed *P* value of less than 0.05 was considered to indicate a statistically significant difference. All statistical analyses were performed using commercially available software (SPSS, version 11, SPSS, Chicago, IL, USA).

Results

Among the 62 nodules showing an atypical pattern on dynamic MRI (set 1), 20 were malignant in 10 patients, accounting for 9.3% of the total nodules and 32% of the atypical nodules in 10/42 patients (23%). Their histological diagnosis was HGDN/early HCC in 20, LGDN in 21, RN in 17 and NRH in 4.

Nineteen out of 20 HGDN/early HCC not characterised by set 1 were only identified as clearly hypointense during the HB-phase (set 2) (mean diameter 14 mm, range 11–19) (Fig. 1), regardless of their dimensions (Fig. 2). Only one histologically confirmed early HCC was missed at set 2, being interpreted as RN because of the absent hypervascularity in the dynamic phase and isointensity in the HB-phase. There were two false-positive results (diagnosed histologically as LGDN) and interpreted as HGDN/early HCC due to their hypointensity in the HB-phase images (Table 1).

The sensitivity of set 1 for HGDN/early HCC (*SCORE 1*) was 88.4% (153/173),raised to 99.4% (172/173) by the combined reading of dynamic and HB-phases (set 2) (Table 2). The specificity of set 1 was 88% (37/42) and that of set 2 was 95% (40/42). The diagnostic accuracy was 88% (190/215) for set 1 and 98.5% for set 2 (212/215). The

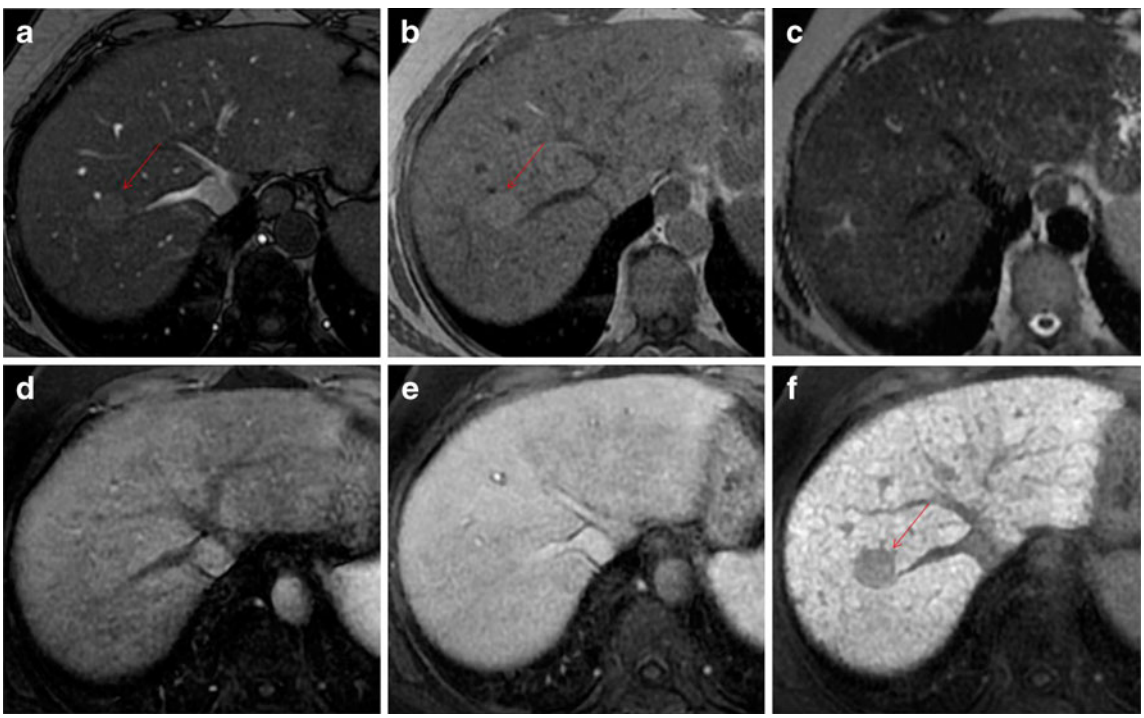

Fig. 1 Gd-EOB-DTPA-enhanced MR images in a 52-year-old man with histologically confirmed early HCC in the VIII segment. **a**–**c** Pre-contrast MRI: T1-weighted out-of phase (**a**) and in-phase images (**b**) demonstrate a slightly hyperintense nodule of < 2 cm *(arrows)*, appearing isointense on the T2-weighted image (**c**). **d**–**e** Dynamic contrast-enhanced images do not delineate any definite focal lesion in the VIII segment: **d** Arterial phase. **e** Portal-venous phase. **f** Hepatobiliary phase image: 20 mins after Gd-EOB-DTPA bolus injection: the nodule appears highly hypointense (no uptake of contrast agent) compared with the surrounding enhanced liver *(arrow)*

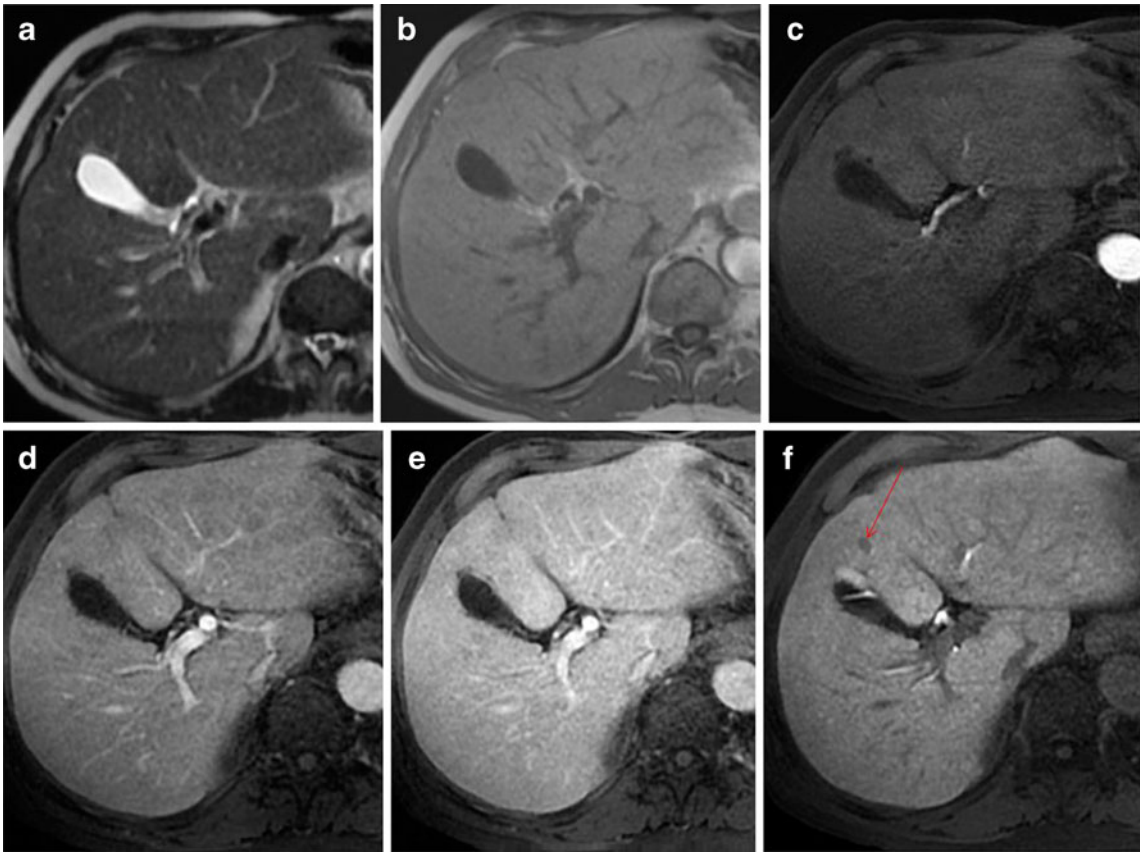

Fig. 2 Gd-EOB-DTPA-enhanced MR images in a 47-year-old woman with histologically proven HGDN in the IV segment. **a**–**b** Pre-contrast T2-weighted (**a**) and T1-weighted (**b**) sequences do not demonstrate definite focal lesions. **c**–**e** In the arterial (**c**), portal venous (**d**) and delayed (**e**) phases there is still no evidence of focal lesions. In the hepatobiliary phase (**f**) 20 mins after Gd-EOB-DTPA bolus injection, a subcentimetric nodule (8 mm) is detected, appearing highly hypointense *(arrow)*

PPV of set 1 was 97% (153/158) and that of set 2 was 99% (172/174). The low NPV of set 1, 65%, (37/57) was substantially increased in set 2 up to 97.5% (40/41).

Although statistically not significant, the addition of HB-phase images provided an added value of 11% in sensitivity (P=0.45), 7% in specificity (P=0.81), 10.5% in diagnostic accuracy (P=0.43), 2% in PPV (P=0.89), and 32.5% in NPV (P=0.18). The combined reading of both sets increased the diagnostic confidence of the readers, particularly because of the highest reliability in excluding malignancy.

The criteria defined as *SCORE 2* identified 36 out of 38 LGDN/RN with 95% sensitivity, whereas *SCORE 3* identified the totality of the confirmed NRH (Fig. 3).

Discussion

Gd-EOB-DTPA is transported into hepatocytes via the organic anion-transporting polypeptide 8 (OATP8) and excreted via the canalicular multi-drug resistant protein 3 (MRP3) [22, 25, 37–39]. OATP8 is typically inhibited in malignant liver lesions, so that they appear hypointense in the HB-phase [22, 36]. Nevertheless, less than 5% of HCCs are imaged as hyperintense in the HB-phase [25, 26, 39], due to intense retention secondary to over-expression of OATP8 and MRP3 [36, 37], but their dynamic vascular pattern has not been described. In the present series, hyperintensity in the HB-phase was only found in 4 nodules (1.9%) and always coupled with arterial hyperintensity and absent washout in the venous phase, showing the typical "focal nodular hyperplasia (FNH)-like" behaviour [41] (Fig. 3). These lesions were correctly diagnosed as NRH. However, it is important to remind that hyperintense nodules in the HB-phase without the typical FNH-like vascular pattern in the dynamic phase may be malignant, especially in cirrhotic livers.

In our population, an atypical vascular behaviour according to AALSD criteria [13–15] was very frequent: 29% of nodules in 33% patients and one third (32%) were malignant (HGDN/early HCC)—the "one-third rule". Hence, the prevalence of hypovascular HCC undetectable by dynamic MRI in our study population was 9.3%.

Table 2 Comparison of sensitivity, specificity, diagnostic accuracy, PPV and NPV between the two sets of MR images for diagnosis of HGDN/early HCC *(Score 1)*

Score 1	Set 1 (%)[a]	Set 2 (%)[a]	P Value[b]
Sensitivity	88.4 (153/173)	99.4 (172/173)	0.45
<1 cm	94 (31/33)	100 (33/33)	0.82
1–2 cm	87 (122/140)	99 (139/140)	0.45
P Value[c]	0.79	0.99	
Specificity	88 (37/42)	95 (40/42)	0.81
<1 cm	80 (4/5)	100 (6/6)	0.99
1–2 cm	91.6 (33/36)	94.4 (34/36)	0.92
P Value	0.99	0.92	
Diagnostic Accuracy	88 (190/215)	98.5 (212/215)	0.43
<1 cm	90 (35/39)	100 (39/39)	0.74
1–2 cm	88 (155/176)	98.3 (173/176)	0.47
P Value	0.92	0.99	
Positive Predictive Value	97 (153/158)	99 (172/174)	0.89
<1 cm	94 (31/33)	100 (33/33)	0.82
1–2 cm	97.6 (122/125)	98.6 (139/141)	0.99
P Value	0.88	0.99	
Negative Predictive Value	65 (37/57)	97.5 (40/41)	0.18
<1 cm	66.6 (4/6)	100 (6/6)	0.99
1–2 cm	64.7 (33/51)	97 (34/35)	0.22
P Value	0.99	0.99	

Set 1: unenhanced (basal T1- and T2-weighted) and Dynamic phases images (arterial-, portal venous- and equilibrium-phases); set 2: unenhanced, Dynamic phases and HB phases (10- and 20-min delayed images).

[a] Numbers in parentheses were used to calculate the percentages.

[b] Difference between the two sets of MR images.

[c] Difference between the two size ranges (<1 cm and 1–2 cm)

The true prevalence of hypovascular "early HCC" is still uncertain, being influenced by the imaging method used. Bolondi et al. [16] reported a prevalence of 17% of hypovascular lesions among tiny (1–2 cm) HCCs at CEUS and CT, but this rate can be lowered when a more sensitive imaging method is used, such as dynamic MRI. More recently, Leoni et al. [8]] have shown that about 20% of these small HCCs do not present the typical vascular pattern at CEUS, CT and dynamic MRI. Namely, 14% of HCCs measuring 10–19 mm did not show a typical vascular pattern coincidentally with two imaging methods and 13% of those of 20–30 mm showed the typical pattern with only one method. Four HCCs ranging from 2 to 3 cm (5%) out of 75 nodules remained undetected by all three dynamic imaging methods, being hypovascular even on dynamic MRI. These results can be explained taking into account that in the initial phases of carcinogenesis, the nodule discloses an arterial hypovascularity with portal perfusion still present and, in the next step, both arterial and portal blood supplies decrease. Only subsequently, intranodular arterial vascularity increases to an isovascular pattern, and finally to a hypervascular pattern [40].

Kogita et al. [26] demonstrated that the decrease in the nodules' portal supply in CT Hepatic Arterial Portography (CTAP) is preceded by the decrease of Gd-EOB-DTPA uptake and that this hepatobiliary agent can help in diagnosing early malignant cirrhotic lesions. Only one case of well-differentiated HCC was recently reported by Ahn et al. [27] displaying a typical vascular pattern at dynamic MRI but appearing isointense in the HB-phase, thus expressing residual hepatocyte activity [44–46]. In our study population, all HCCs with a typical appearance at Dynamic MRI were also confirmed in the HB-phase by the absence of uptake.

In the paper by Kogita [26], among 39 well-differentiated HCCs, 5% were isointense in the HB-phase and among 8 DNs, 37.5% were hypointense, simulating HCCs: however, their pattern at dynamic MRI was not described and their vascular behaviour could have been a diagnostic determinant, as the final diagnosis should rely on the combined reading of both phases.

In the study by Ahn et al. [27], 9 out of 84 HCCs (10.7%) in six patients were exclusively identified by their hypointensity on HB-phase images -and three were early HCCs <1.5 cm-, while in our population 19 out of 20 HGDN/early HCC remained unclassified at dynamic MRI alone because of atypical behaviour (Figs.1, 2) and were diagnosed only in the HB-phase. The pathological explanation of the absent arterial enhancement is the weak development of non-triadal arteries in HGDN/early HCC, making their characterization based on dynamic MR phases impossible [46–49]. These results support the hypothesis that hypointensity in the HB-phase indicates the malignant nature of the lesion [24, 27] and that hypointensity gradually increases as the nodule evolves towards malignancy [25].

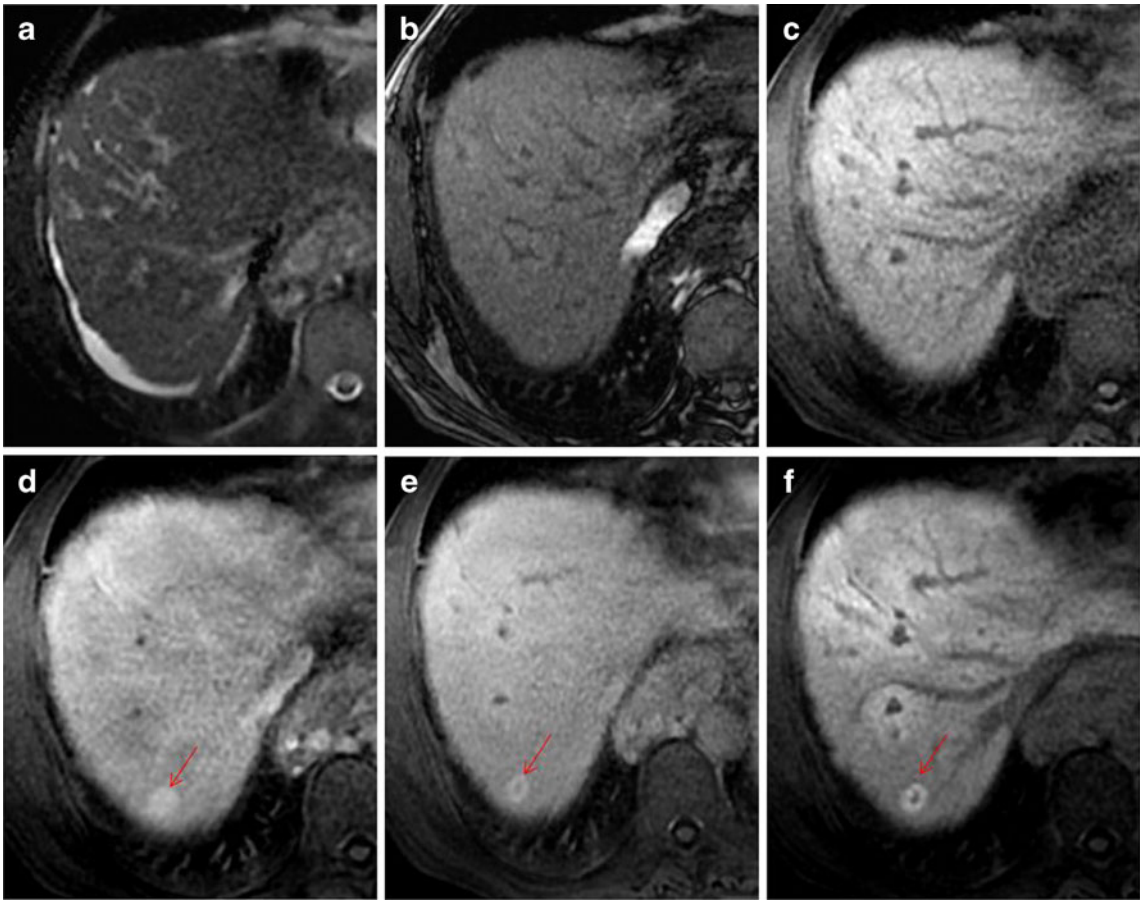

Fig. 3 Gd-EOB-DTPA-enhanced MR images in a 55-year-old man with histologically confirmed NRH in the VII segment. No definite focal lesions were demonstrated on pre-contrast MRI T2-weighted (**a**) and T1-weighted (**b**) images. On GRE 3D T1-weighted (LAVA) images (**c**), the nodule appears slightly hypointense. On Dynamic MRI the lesion is shown as homogeneously enhancing in the arterial phase (**d**), becoming peripherally more hyperintense except for the core of the lesion (**e**). In the hepatobiliary phase (**f**) after 20 min, the lesion appears highly hyperintense, with an FNH-like appearance: peripheral uptake of the contrast agent and hypointense central scar

In our series, on the combined reading of dynamic and HB-phase images (set 2) there was only one false-negative early HCC, interpreted as RN because of both isovascularity in the dynamic phase and isointensity in the HB-phase. This pattern can be observed in well-differentiated HCCs with a poor development of non-triadal arteries combined with residual hepatocyte activity, allowing a delayed uptake of the contrast material [44–46].

Gd-BOPTA-enhanced MRI with both dynamic and HB-phase studies for lesions of <2 cm has shown a 63% detection rate [50], and a maximum of 76% sensitivity, further decreasing to a maximum sensitivity of 43% for HCCs of <1 cm [31]. Gd-EOB-DTPA-enhanced MRI demonstrated a higher (86%) sensitivity for HCCs of ≤2 cm, although tested on a small population (n=35) [51].

In our series, the dynamic MR phase (set 1) demonstrated 88.4% sensitivity, higher than the maximum rate of 75% referred to by Ahn et al. [27], despite the same contrast medium and the same HCC size (<2 cm) chosen in the two studies.

In our experience, the addition of the HB-phase to dynamic MRI improved sensitivity up to 99.4%, with a net gain of 11% in the detection rates of HGDN/early HCC of <2 cm: similarly, a maximum increase in sensitivity from 85.7% to 91.7% was referred to by Ahn et al. [27] and a gain of 13%—from 50% to 63%—in sensitivity was reported by Marin et al. [50] by using Gd-BOPTA.

Instead, PPV was not affected by the addition of the HB-phase (varying from 97 to 99%) as already reported by Marin [50], in which PPV moved to 97% from 93%. Conversely, the combined reading strongly influences the NPV, which increased by 32.5% (until 97.5%) compared with dynamic MRI alone (65%). This result, although statistically not significant, is important for the management of cirrhotic patients, who run a high risk of developing malignant nodules.

Our study has some limitations. Taking into account that the sensitivity of any test is increased by a higher pre-test prevalence of the disease [51–53], it is pertinent to note that

our population only included cirrhotic patients periodically screened with US and referred for MR examination when HCC was suspected. Our patients had, therefore, a rather high chance of bearing a malignant nodule, as confirmed by the low prevalence of non-HCC lesions we observed. Nonetheless, this scenario reflects the best current clinical practice for patients at risk of HCC.

Another limitation is that we might have missed a substantial number of lesions because we did not have pathological assessment of the whole liver, with the exception of the 11 transplanted patients. Moreover, although all patients had at least one pathologically confirmed lesion, the histological assessment was not possible for nodules only visible on MRI. Therefore, the high detection rates reported in this study represent relative, not absolute, sensitivities. However, the main purpose of our study was not to test the absolute sensitivity of dynamic MRI and HB-phase separately, but to evaluate the added value of the HB-phase to dynamic MRI in the same sample population.

Furthermore, in the same category of malignant nodules (score 1) we artificially considered both early HCC and HGDN, assuming that these two entities cannot be distinguished at imaging and both are frequently atypical at dynamic studies. Our choice is in line with the pathological debate concerning these lesions. In Japan, ≤2 cm HCCs are categorized in two types: "distinctly nodular" (usually hypervascular at imaging) and "indistinctly/vaguely nodular" (non-hypervascular) [17, 42, 45, 54–56]. However, the possibility to achieve a clear distinction of the latter HCCs from HGDNs is still debated with Western pathologists, who tend to diagnose them as HGDNs [43].

In conclusion, given the high incidence of atypical nodules (33% of patients) in our series together with a high rate of malignant nodules (32%) among these (the "one-third rule"), an extensive employment of Gd-EOB-DTPA-enhanced MRI can be suggested in the follow-up of small nodules detected on surveillance US. In our institution, Gd-EOB-DTPA is currently the first choice of contrast agent in liver MR studies for evaluating these lesions, because the HB-phase assists in better diagnosing early HCCs, which have a high chance of being cured and a low risk of recurrence [57, 58].

Acknowledgment Antonio Di Micoli M.D., Division of Internal Medicine, Department of Digestive Diseases and Internal Medicine; Sant' Orsola-Malpighi Hospital, University of Bologna, Bologna, Italy for the support in the statistical analysis

References

1. Sherman M (2010) Epidemiology of hepatocellular carcinoma. Oncology 78(Suppl 1):7–10
2. Roayaie S, Llovet JM (2005) Liver transplantation for hepatocellular carcinoma: is expansion of criteria justified? Clin Liver Dis 9:315–28
3. Shibuya K, Yano E (2005) Regression analysis of trends in mortality from hepatocellular carcinoma in Japan, 1972–2001. Int J Epidemiol 34:397–402
4. El-Serag HB (2004) Hepatocellular carcinoma: recent trends in the United States. Gastroenterology 127:S27–34
5. El-Serag HB, Mason AC (1999) Rising incidence of hepatocellular carcinoma in the United States. N Engl J Med 11:745–750
6. Hayashi M, Matsui O, Ueda K, Kawamori Y, Gabata T, Kadoya M (2002) Progression to hypervascular hepatocellular carcinoma: correlation with intranodular blood supply evaluated with CT during intrarterial injection of contrast material. Radiology 225:143–149
7. Hayashi M, Matsui O, Ueda K, Kawamori Y, Kadoya M, Yoshikawa J, Gabata T, Takashima T, Nonomura A, Nakanuma Y (1999) Correlation between the blood supply and grade of malignancy of hepatocellular nodules associated with liver cirrhosis: evaluation by CT during intraarterial injection of contrast medium. AJR Am J Roentgenol 172:969–976
8. Leoni S, Piscaglia F, Golfieri R, Camaggi V, Vidili G, Pini P, Bolondi L (2010) The impact of vascular and non vascular findings on the non invasive diagnosis of small hepatocellular carcinoma based on EASL and AASLD criteria. Am J Gastroenterol 105:599–609
9. Colli A, Fraquelli M, Casazza G, Massironi S, Colucci A, Conte D, Duca P (2006) Accuracy of ultrasonography, spiral CT, magnetic resonance, and alpha-fetoprotein in diagnosing hepatocellular carcinoma: a systematic review. Am J Gastroenterol 101:513–523
10. Hecht EM, Holland AE, Israel GM, Hahn WY, Kim DC, West AB, Babb JS, Taouli B, Lee VS, Krinsky GA (2006) Hepatocellular carcinoma in the cirrhotic liver: gadolinium-enhanced 3D T1-weighted MR imaging as a stand-alone sequence for diagnosis. Radiology 239:438–447
11. Rode A, Bancel B, Douek P, Chevallier M, Vilgrain V, Picaud G, Henry L, Berger F, Bizollon T, Gaudin JL, Ducerf C (2001) Small nodule detection in cirrhotic livers: evaluation with US, spiral CT, and MRI and correlation with pathologic examination of explanted liver. J Comput Assist Tomogr 25:327–336
12. Snowberger N, Chinnakotla S, Lepe RM, Peattie J, Goldstein R, Klintmalm GB, Davis GL (2007) Alpha fetoprotein, ultrasound, computerized tomography and magnetic resonance imaging for detection of hepatocellular carcinoma in patients with advanced cirrhosis. Aliment Pharmacol Ther 26:1187–1194
13. Bruix J, Sherman M (2005) Management of hepatocellular carcinoma. AASLD PRACTICE GUIDELINE. Hepatology 42:1208–1235
14. Marrero JA, Hussain HK, Nghiem HV, Umar R, Fontana RJ, Lok AS (2005) Improving the prediction of hepatocellular carcinoma in cirrhotic patients with an arterially-enhancing liver mass. Liver Transpl 11:281–289
15. Bruix J, Sherman M (2010) Management of hepatocellular carcinoma: an update. AASLD PRACTICE GUIDELINE. Hepatology July, published online by American Association for the Study of Liver Diseases.http://www.aasld.org/practiceguidelines/Documents/Bookmarked%20Practice%20Guidelines/HCCUpdate2010.pdf
16. Mion F, Grozel L, Boillot O, Paliard P, Berger F (1996) Adult cirrhotic liver explants: precancerous lesions and undetected small hepatocellular carcinomas. Gastroenterology 111:1587–1592
17. Bolondi L, Gaiani S, Celli N, Golfieri R, Grigioni WF, Leoni S, Venturi AM, Piscaglia F (2005) Characterization of small nodules in cirrhosis by assessment of vascularity: the problem of hypovascular hepatocellular carcinoma. Hepatology 42:27–34
18. International Consensus Group for Hepatocellular Neoplasia (2009) Pathologic diagnosis of early hepatocellular carcinoma: a

report of the International Consensus Group for Hepatocellular Neoplasia. Hepatology 49:658–664
19. Spinazzi A, Lorusso V, Pirovano G, Kirchin M (1999) Safety, tolerance, biodistribution, and MR imaging enhancement of the liver with gadobenate dimeglumine: results of clinical pharmacologic and pilot imaging studies in nonpatient and patient volunteers. Acad Radiol 6:282–291
20. Kirchin MA, Pirovano GP, Spinazzi A (1998) Gadobenate dimeglumine (Gd-BOPTA). An overview. Invest Radiol 33:798–809
21. Seale MK, Catalano OA, Saini S, Hahn PF, Sahani DV (2009) Hepatobiliary-specific MR contrast agents: role in imaging the liver and biliary tree. RadioGraphics 29:1725–1748
22. Reimer P, Rummeny EJ, Shamsi K, Balzer T, Daldrup HE, Tombach B, Hesse T, Berns T, Peters PE (1996) Phase II clinical evaluation of Gd-EOB-DTPA: dose, safety aspects, and pulse sequence. Radiology 199:177–183
23. Vogl TJ, Kümmel S, Hammerstingl R, Schellenbeck M, Schumacher G, Balzer T, Schwarz W, Müller PK, Bechstein WO, Mack MG, Söllner O, Felix R (1996) Liver tumors: comparison of MR imaging with Gd-EOB-DTPA and Gd-DTPA. Radiology 200:59–67
24. Saito K, Kotake F, Ito N, Ozuki T, Mikami R, Abe K, Shimazaki Y (2005) Gd-EOB-DTPA enhanced MRI for hepatocellular carcinoma: quantitative evaluation of tumor enhancement in hepatobiliary phase. Magn Reson Med Sci 4:1–9
25. Kim JI, Lee JM, Choi JY, Kim YK, Kim SH, Lee JY, Han JK, Choi BI (2008) The value of gadobenate dimeglumine-enhanced delayed phase MR imaging for characterization of hepatocellular nodules in the cirrhotic liver. Invest Radiol 43:202–210
26. Kogita S, Imai Y, Okada M, Kim T, Onishi H, Takamura M, Fukuda K, Igura T, Sawai Y, Morimoto O, Hori M, Nagano H, Wakasa K, Hayashi N, Murakami T (2010) Gd-EOB-DTPA-enhanced magnetic resonance images of hepatocellular carcinoma: correlation with histological grading and portal blood flow. Eur Radiol 20:2405–2413
27. Ahn SS, Kim MJ, Lim JS, Hong HS, Chung YE, Choi JY (2010) Added value of gadoxetic acid-enhanced hepatobiliary phase MR imaging in the diagnosis of hepatocellular carcinoma. Radiology 255:459–466
28. Forty-first World Medical Assembly (1990) Declaration of Helsinki: recommendations guiding physicians in biomedical research involving human subjects. Bull Pan Am Health Organ 24:606–609
29. International Working Party (1995) Terminology of nodular hepatocellular lesions. Hepatology 22:983–993
30. Stevens WR, Gulino SP, Batts KP, Stephens DH, Johnson CD (1996) Mosaic pattern of hepatocellular carcinoma: histologic basis for a characteristic CT appearance. J Comput Assist Tomogr 20:337–342
31. Choi SH, Lee JM, Yu NC, Suh KS, Jang JJ, Kim SH, Choi BI (2008) Hepatocellular carcinoma in liver transplantation candidates: detection with gadobenate dimeglumine-enhanced MRI. AJR Am J Roentgenol 191:529–536
32. Kim YK, Kwak HS, Han YM, Kim CS (2007) Usefulness of combining sequentially acquired gadobenate dimeglumine-enhanced magnetic resonance imaging and Resovist enhanced magnetic resonance imaging for the detection of hepatocellular carcinoma: comparison with computed tomography hepatic arteriography and computed tomography arterioportography using 16-slice multidetector computed tomography. J Comput Assist Tomogr 31:702–711
33. Willatt JM, Hussain HK, Adusumilli S, Marrero JA (2008) MR Imaging of hepatocellular carcinoma in the cirrhotic liver: challenges and controversies. Radiology 247:311–330
34. Brancatelli G, Federle MP, Grazioli L, Golfieri R, Lencioni R (2002) Large regenerative nodules in Budd-Chiari Syndrome and other vascular disorders of the liver: CT and MR imaging findings with clinicopathologic correlation. AJR Am J Roentgenol 178:877–883
35. Amesa JT, Federle MP, Chopra K (2009) Distinguishing clinical and imaging features of nodular regenerative hyperplasia and large regenerative nodules of the liver. Clin Radiol 64:1190–1195
36. Kitao A, Zen Y, Matsui O, Gabata T, Kobayashi S, Koda W, Kozaka K, Yoneda N, Yamashita T, Kaneko S, Nakanuma Y (2010) Hepatocellular carcinoma: signal intensity at gadoxetic acid–enhanced MR imaging—correlation with molecular transporters and histopathologic features. Radiology 256:817–826
37. Narita M, Hatano E, Arizono S, Miyagawa-Hayashino A, Isoda H, Kitamura K, Taura K, Yasuchika K, Nitta T, Ikai I, Uemoto S (2009) Expression of OATP1B3 determines uptake of Gd-EOB-DTPA in hepatocellular carcinoma. J Gastroenterol 44:793–798
38. Pascolo L, Petrovic S, Cupelli F, Bruschi CV, Anelli PL, Lorusso V, Visigalli M, Uggeri F, Tiribelli C (2001) Abc protein transport of MRI contrast agents in canalicular rat liver plasma vesicles and yeast vacuoles. Biochem Biophys Res Commun 282:60–66
39. Hamm B, Staks T, Mühler A, Bollow M, Taupitz M, Frenzel T, Wolf KJ, Weinmann HJ, Lange L (1995) Phase I clinical evaluation of Gd-EOB-DTPA as a hepatobiliary MR contrast agent: safety, pharmacokinetics, and MR imaging. Radiology 195:785–792
40. Kudo M (2008) Hepatocellular carcinoma 2009 and beyond: from the surveillance to molecular targeted therapy. Oncology 75(suppl 1):1–12. doi:10.1159/000181865
41. Hammerstingl R, Huppertz A, Breuer J, Balzer T, Blakeborough A, Carter R, Fusté LC, Heinz-Peer G, Judmaier W, Laniado M, Manfredi RM, Mathieu DG, Müller D, Mortelè K, Reimer P, Reiser MF, Robinson PJ, Shamsi K, Strotzer M, Taupitz M, Tombach B, Valeri G, van Beers BE, Vogl TJ, European EOB-study group (2008) Diagnostic efficacy of gadoxetic acid (Primovist)-enhanced MRI and spiral CT for a therapeutic strategy: comparison with intraoperative and histopathologic findings in focal liver lesions. Eur Radiol 18(3):457–467. doi:10.1007/s00330-007-0716-9
42. Tajima T, Honda H, Taguchi K, Asayama Y, Kuroiwa T, Yoshimitsu K, Irie H, Aibe H, Shimada M, Masuda K (2002) Sequential hemodynamic change in hepatocellular carcinoma and dysplastic nodules: CT angiography and pathologic correlation. AJR Am J Roentgenol 178:885–897
43. Kojiro M (2007) Diagnostic discrepancy of early hepatocellular carcinoma between Japan and West. Hepatology Res 37:S249–S252
44. Gabata T, Matsui O, Kadoya M, Yoshikawa J, Ueda K, Kawamori Y, Takashima T, Nonomura A (1998) Delayed MR imaging of the liver: correlation of delayed enhancement of hepatic tumors and pathologic appearance. Abdom Imaging 23:309–313
45. Grazioli L, Morana G, Caudana R, Benetti A, Portolani N, Talamini G, Colombari R, Pirovano G, Kirchin MA, Spinazzi A (2000) Hepatocellular carcinoma: correlation between gadobenate dimeglumine-enhanced MRI and pathologic findings. Invest Radiol 35:25–34
46. Manfredi R, Maresca G, Baron RL, Cotroneo AR, De Gaetano AM, De Franco A, Pirovano G, Spinazzi A, Marano P (1999) Delayed MR imaging of hepatocellular carcinoma enhanced by gadobenate dimeglumine (Gd-BOPTA). J Magn Reson Imaging 9:704–710
47. Nakashima Y, Nakashima O, Hsia CC, Kojiro M, Tabor E (1999) Vascularization of small hepatocellular carcinomas: correlation with differentiation. Liver 19:12–18
48. Takayasu K, Furukawa H, Wakao F, Muramatsu Y, Abe H, Terauchi T, Winter TC 3rd, Sakamoto M, Hirohashi S (1995) CT

diagnosis of early hepatocellular carcinoma: sensitivity, findings, and CT-pathologic correlation. AJR Am J Roentgenol 164:885–890
49. Lim JH, Choi D, Kim SH, Lee SJ, Lee WJ, Lim HK, Kim S (2002) Detection of hepatocellular carcinoma: value of adding delayed phase imaging to dual-phase helical CT. AJR Am J Roentgenol 179:67–73
50. Marin D, Di Martino M, Guerrisi A, De Filippis G, Rossi M, Ginanni Corradini S, Masciangelo R, Catalano C, Passariello R (2009) Hepatocellular carcinoma in patients with cirrhosis: qualitative comparison of gadobenate dimeglumine-enhanced MR imaging and multiphasic 64-section CT. Radiology 251:85–95
51. Kim SH, Kim SH, Lee J, Kim MJ, Jeon YH, Park Y, Choi D, Lee WJ, Lim HK (2009) Gadoxetic acid-enhanced MRI versus triple-phase MDCT for the preoperative detection of hepatocellular carcinoma. AJR Am J Roentgenol 192:1675–1681
52. Ransohoff DF, Feinstein AR (1978) Problems of spectrum and bias in evaluating the efficacy of diagnostic tests. N Engl J Med 299:926–930
53. Bossuyt PM, Reitsma JB, Bruns DE, Gatsonis CA, Glasziou PP, Irwig LM, Moher D, Rennie D, de Vet HC, Lijmer JG (2003) Standards for reporting of diagnostic accuracy. The STARD statement for reporting studies of diagnostic accuracy: explanation and elaboration. Ann Intern Med 138:W1–12
54. Kojiro M (2004) Focus on dysplastic nodules and early hepatocellular carcinoma: an Eastern point of view. Liver Transpl 10:S3–S8
55. Kojiro M, Roskams T (2005) Early hepatocellular carcinoma and dysplastic nodules. Semin Liver Dis 25:133–142
56. Kudo M (2009) Multistep human hepatocarcinogenesis: correlation of imaging with pathology. J Gastroenterol 44:112–118
57. Inoue K, Takayama T, Higaki T, Watanabe Y, Makuuchi M (2004) Clinical significance of early hepatocellular carcinoma. Liver Transpl 10:S16–S19
58. Yamamoto M, Takasaki K, Otsubo T, Katsuragawa H, Katagiri S, Yoshitoshi K, Ariizumi S, Saito A, Nakano M (2004) Favorable surgical outcomes in patients with early hepatocellular carcinoma. Ann Surg 239:395–399